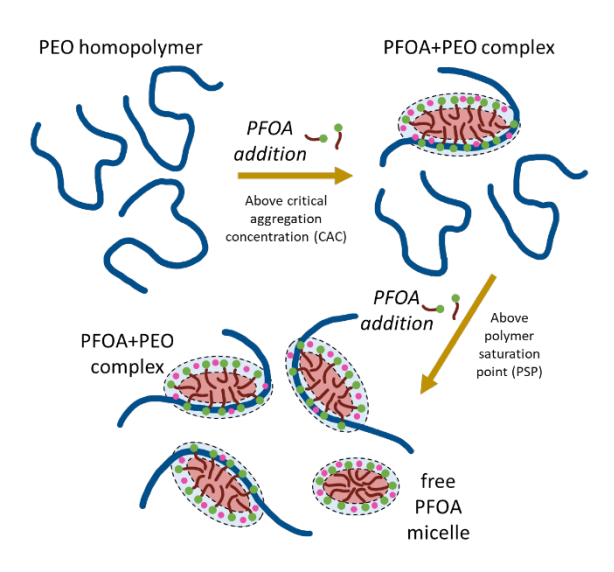
# Binding of Perfluorooctanoate to Poly(ethylene oxide)

Samhitha Kancharla,<sup>1</sup> Dengpan Dong,<sup>2</sup> Dmitry Bedrov,<sup>2</sup> \* Paschalis Alexandridis,<sup>1</sup> \* Marina Tsianou <sup>1</sup> \*

1 Department of Chemical and Biological Engineering, University at Buffalo, The State University of New York (SUNY), Buffalo, NY 14260-4200, U.S.A.

2 Department of Materials Science and Engineering, University of Utah, 122 South Central Campus Drive, Room 304, Salt Lake City, UT 84112, U.S.A.



Corresponding authors: Marina Tsianou <a href="mailto:mtsianou@buffalo.edu">mtsianou@buffalo.edu</a>, Paschalis Alexandridis <a href="mailto:palexand@buffalo.edu">palexand@buffalo.edu</a>, and Dmitry Bedrov <a href="mailto:d.bedrov@utah.edu">d.bedrov@utah.edu</a>

**ABSTRACT** 

To inform the design of polymer-based adsorbent materials for sequestration of per- and

polyfluoroalkyl substances (PFAS) from aqueous solution, we report here on the critical

aggregation concentration (CAC), shape, size, composition, and interactions of assemblies

formed in water between perfluorooctanoic acid ammonium salt (PFOA) and the nonionic

polymer poly(ethylene oxide) (PEO), obtained from complementary experiments (conductivity,

surface tension, pyrene fluorescence, viscosity, and small-angle neutron scattering (SANS)) and

atomistic molecular dynamics (MD) simulations. PEO-PFAS binding commences at

concentrations lower than the PFOA critical micelle concentration (CMC), and is driven by PEO

localizing on the micelle surface and shielding the fluorocarbon parts of PFOA from contact with

water. PFOA+PEO mixed micelles have 10% higher association number and are 40% more

elongated compared to polymer-free PFOA micelles. This is the first investigation on the

structure of polymer+fluorocarbon surfactant mixed micelles, and contributes fundamental

insights on the association of water-soluble polymers with PFAS surfactants.

Keywords: polyethylene glycol, PEG, micelle, PFAS, PFOA, remediation

2

### INTRODUCTION

received much attention owing to their extensive application in many industrial formulations. 1-5 Anionic surfactants such as sodium dodecylsulfate (SDS) interact with nonionic polymers such as poly(ethylene oxide) (PEO) in aqueous solutions above a certain concentration called the critical association (or aggregation) concentration (CAC), which is typically much lower than the critical micellization concentration (CMC) of the surfactant in the absence of a polymer. 1, 2, 6, 7 With an increase in the surfactant concentration comes a certain polymer saturation point (PSP) where the polymer chains become saturated with bound surfactant and, above the PSP, surfactant micelles that are free, i.e., not associated with polymer, begin to form.<sup>1, 2, 6</sup> The generally accepted picture for the association between PEO and surfactants is that of surfactant micelles bound along the PEO chain in a pearl-necklace configuration.<sup>6, 8-12</sup> The interactions between polymers and surfactants depend highly on their relative charge and the hydrophobicity. 1, 13-17 Surfactants containing a fluorinated hydrophobic tail and a hydrophilic headgroup are a major subgroup of per- and polyfluoroalkyl substances (PFAS) also known as "Forever Chemicals". The strong C-F bond, weak -CF<sub>2</sub>- intermolecular forces and strong hydrophobic interactions result in outstanding properties of fluorinated surfactants, including incompatibility with both water and oil, high surface wetting ability, strong surface activity, and high chemical and thermal stability compared to hydrocarbon surfactants. 18-20 These properties render fluorinated surfactants useful in niche applications, including nonstick cookware, food packaging paper, stain repellant and waterproof clothing, paints, cosmetics, and firefighting foams. 21-25 For these reasons, perfluorooctanoate (PFOA) and perfluorooctane sulfonate (PFOS) were widely used globally, but now they are banned. The widespread usage of PFAS surfactants in industrial

Surfactant and polymer interactions and the various structures formed in aqueous solution have

processes and consumer products has resulted in their release into the environment, and they accumulate in drinking, waste, and marine water, leach to the groundwater, adsorb to soil and sediments, become volatilized, and/or are taken up in plants and biota.<sup>26-30</sup> PFAS surfactants can enter the human body through water and food that get contaminated from contact with PFAS-treated packaging or cookware,<sup>31,32</sup> and can cause adverse health effects.<sup>29,32,33</sup>

These findings necessitate the removal of PFAS present in the aquatic environment. A promising technology for removing PFAS surfactants from water is adsorption using materials such as activated carbon, minerals, ion exchange resins, and polymer networks. <sup>20, 30, 34-38, 39</sup> For the design of effective and selective adsorbent materials for PFAS removal, a fundamental understanding of the molecular organization and various interactions of PFAS with polymers is crucial.

Binding of fluorinated surfactants to PEO at rather low concentrations (~0.1 wt%) in aqueous solution has been probed using isothermal titration calorimetry (ITC), NMR, density, viscosity, surface tension, and conductivity. The available literature shows fluorinated surfactants to bind to PEO at concentrations lower than their CMC in water in the absence of polymer. ITC data of perfluoroalkyl carboxylate+PEO systems have been used to calculate thermodynamic parameters for the association of surfactant micelles on a PEO chain under the approximation of the pseudo-phase model. According to the authors, "the lack of structural data on the aggregation number of the perfluoroalkanoate-PEG aggregates prevents a more quantitative analysis of the present thermodynamic data".

Direct structural information on the complexes formed between fluorinated surfactants and PEO is not available in the literature, but can be obtained by small-angle neutron scattering (SANS), as has been the case for SDS+PEO complexes.<sup>6, 8-11</sup> It has been proposed that the association of

PFOA or SDS micelles on a PEO chain is driven by hydrophobic interactions, but the dominant effect is entropic in the case of SDS, while enthalpic for PFOA.<sup>40, 42, 44</sup> For SDS+PEO, this is supported by molecular dynamics (MD) simulations,<sup>12</sup> however, no such studies are available for aqueous solutions of fluorinated surfactants and polymers. MD simulations can, not only offer insights into the governing interaction and allow us to test the association mechanisms suggested in previous experimental studies, but also provide valuable information on the structure.

This study probes assemblies (mixed micelles) formed by PFOA and PEO homopolymer in aqueous solutions. To this end, complementary experimental measurements (conductivity, surface tension, pyrene fluorescence, viscosity, and small-angle neutron scattering (SANS)) and atomistic MD simulations are analyzed to determine the CAC, shape, size, and interactions of PFOA+PEO mixed micelles, conformation and location of PEO chains in PFOA+PEO mixed micelles, and the effects of surfactant and polymer concentration. To the best of our knowledge, this is the first investigation on the structure of polymer+PFAS surfactant mixed micelles.

### MATERIALS AND METHODS

### Materials

Ammonium perfluorooctanoate (PFOA), (C<sub>7</sub>F<sub>15</sub>COONH<sub>4</sub>, CAS number: 3825-26-1, MW = 431.1 g/mol, 98% purity), also known as pentadecafluorooctanoic acid ammonium salt, was obtained from SynQuest Laboratories (Alachua, FL, USA). Poly(ethylene oxide) (PEO) (BioUltra 10000, MW = 8500-11500) was obtained from Sigma Life Science (St. Louis, MO, USA). Deuterium oxide (D, 99.9%), (D<sub>2</sub>O, MW = 20.03 g/mol, 99.5% purity) was obtained from Cambridge Isotope Laboratories, Inc. (Tewksbury, MA, USA) and used as received. Samples used in SANS were prepared using D<sub>2</sub>O. Samples tested with other techniques were prepared using Milli-Q purified water (0.055  $\mu$ S/cm). To prepare surfactant+polymer solutions of various surfactant concentrations, an aqueous solution of the required PEO concentration was prepared first, and the dry surfactant was then added to this solution. All samples were allowed sufficient time to equilibrate following the mixing of ingredients.

Ammonium perfluorooctanoate was selected in this study as it is the most widely used among other perfluorooctanoate salts, and the most widespread PFO contaminant in the environment.<sup>28</sup> Another notorious PFAS surfactant contaminant, GenX,<sup>45</sup> is available commercially only as ammonium salt, and not in other salts. PEO was selected as a commercially available and environment friendly polymer that has been shown to associate with ionic surfactants in aqueous solutions. The relatively short PEO molecular weight was selected with an adsorbent material in mind, where PEO chains tethered on surfaces will present sites for PFAS surfactant association and accumulation.

The concentration of PEO 10000 used in the experiments is 3 wt%. The overlap concentration calculated from C\*=  $MW/(4\pi R_g^3 N_{AV}/3)$  x 100 is found C\* = 21 wt%, thus we operate well below the C\*. The radius of gyration ( $R_g = 26.7$  Å) value used in the above C\* calculation has been obtained from the Guinier model fitting to SANS data of 3% PEO 10000 in D<sub>2</sub>O (refer to SI). The concentration range of PFOA studied here is 0 – 150 mM. SANS measurements of 3% PEO 10000 + PFOA were performed at concentrations 33 mM and 110 mM PFOA.

# **Experimental Characterization**

Conductivity: Conductivity experiments for PFOA + PEO aqueous solutions were performed and analyzed as described in the Supporting Information (SI) document and in references. <sup>13, 46</sup> For nonionic polymer + ionic surfactant mixed systems at fixed polymer concentration, the conductivity vs surfactant concentration curve exhibits two break points: (i) concentration where the surfactant starts binding to the polymer: critical association concentration (CAC), <sup>47, 48</sup> and (ii) concentration (C<sub>m</sub>) where free surfactant micelles start to form in the aqueous solution after the polymer has been saturated by surfactant. <sup>47, 48</sup> For PFOA + PEO systems, two linear regions with one break point were observed in the conductivity vs surfactant concentration plots. <sup>47</sup> The higher concentration break point is not observed here because free PFOA micelles form above the PFOA concentration range (1 – 45 mM) considered in our conductivity plots.

Surface tension: The surface tension of aqueous PFOA + PEO solutions was measured, and the results analyzed as described in the SI document and in references. 13, 46

*Micropolarity:* The micropolarity of PFOA aqueous solutions in the absence and in the presence of PEO is probed using pyrene fluorescence spectroscopy. Details on the experiment procedure

and analysis of results are described in SI and references.<sup>13, 46, 49</sup> Information on the critical concentrations for different PEO+surfactant solutions was obtained here from the point where  $I_1/I_3$  starts to decrease following a plateau region in the  $I_1/I_3$  vs. surfactant concentration curve.

Viscosity: The viscosity experiments for PFOA + PEO aqueous solutions were performed and the relative viscosity ( $\eta_{rel}$ ) of the solution calculated as described in SI and references.<sup>13, 46</sup>

Small-angle neutron scattering (SANS): SANS measurements of aqueous PFOA solutions in the absence and in the presence of PEO were performed on the NG-B 30 m SANS instrument at the Center for Neutron Research (NCNR), National Institute of Standards and Technology (NIST), Gaithersburg, MD (refer to SI for information on SANS data collection and reduction). SANS has been widely used to determine the size and structure of surfactant micelles.<sup>6,49-56</sup>

SANS data were collected for 3% PEO 10000 in D<sub>2</sub>O (no surfactant), and 33.3 mM or 110 mM PFOA + 3% PEO 10000 in D<sub>2</sub>O. Since 3% PEO falls well within the dilute concentration regime, the correlation length model or Debye Gaussian model can be applied to fit the SANS data of 3% PEO 10000 in D<sub>2</sub>O (refer to SI for details).<sup>6,57,58</sup>

The scattering intensities from PFOA + PEO mixed micelles are fitted using a combination of the core-shell ellipsoid form factor and Hayter rescaled mean spherical approximation (RMSA) structure factor with the correlation length model. The core-shell ellipsoid form factor and Hayter RMSA structure factor (details are provided in the subsequent text) have been widely used for describing ionic surfactant micelles.<sup>6, 49, 53, 54</sup> The correlation length model is incorporated to the overall scattering intensity to account for scattering (at low-q values) originating from a fraction of polymer molecules that are not forming complexes with PFOA and thus cannot be described by the core-shell form factor.<sup>15</sup> The correlation length model is a

combination of Lorentzian and power law terms, and has been previously used to capture the scattering originating from nonionic polymers in aqueous solution.<sup>6, 59</sup> The power law term describes Porod scattering from clusters, capturing the scattering behavior at low-q values. The Lorentzian term describes scattering from polymer chains and captures the scattering behavior at high-q.<sup>6, 59</sup> The overall scattering intensity I(q) is then given by:

$$I(q) = scale_1 I(q)_1 + scale_2 I(q)_2 + B_{inc}$$
 (1)

where  $I(q)_1$  is the intensity from the correlation length model which is calculated as:

$$I(q)_1 = \frac{A}{q^n} + \frac{C}{1 + (q\xi)^m}$$
 (2)

The first term of I(q)<sub>1</sub> describes the Porod scattering from clusters with the power law exponent n capturing the scattering behavior at low q values. n reflects the mass fractal dimension of the clusters, and the scale factor A the scattering contribution of clusters. Clustering has been observed in many macromolecular solutions, however, its origin has remained elusive.<sup>59</sup> Note that the low-q range examined in our SANS data captures only a small portion of the scattering originating from clusters. Hence, the cluster size cannot be determined from the present data.<sup>59</sup>

The second term of  $I(q)_1$  is a Lorentzian function describing scattering from polymer chains (exponent = m) which characterizes the polymer/solvent interactions. The correlation length  $\xi$  is related to the radius of gyration of a single Gaussian polymer chain at intermediate q values:  $R_g = \sqrt{2}\xi$ . The scale factor C captures the solvation scattering of the polymer: a lower C value indicates more effective solvation.

I(q)<sub>2</sub> is the intensity from the core-shell ellipsoid form factor and the Hayter – Penfold structure factor with rescaled mean spherical approximation (RMSA). The expressions describing the form factor and structure factor models, are presented in SI.

Table S1 (in SI) lists the parameters (in the SASview software) that have been used here in fitting SANS data from PFOA + PEO systems for the combination of the correlation length model with the core-shell ellipsoid form factor and Hayter MSA structure factor.

We considered in this analysis one PFOA micelle per PEO 10000 chain (at 3 wt% PEO), based on information from SANS available on SDS-PEO complexes formed at much higher PEO MW and much lower PEO concentration, which suggested 10 SDS micelles per PEO 135000 chain (at 0.1 wt% PEO) and 6 SDS micelles per PEO 90000 chain (at 0.5 wt% PEO).<sup>6,8</sup>

Two different scenaria for describing the composition of PFOA + PEO mixed micelles have been considered in the analysis of SANS data:

- dry micelle core consisting of PFOA CF<sub>3</sub>(CF<sub>2</sub>)<sub>6</sub> fluorocarbon chains (no polymer, no water), and micelle shell comprising PFOA headgroups, counterions, EO segments and associated water of hydration, while the remaining EO segments are in the bulk solution;
- dry micelle core consisting of PFOA CF<sub>3</sub>(CF<sub>2</sub>)<sub>5</sub> chains (no polymer, no water), and micelle shell comprising 1 CF<sub>2</sub> group of PFOA, PFOA headgroups, counterions, EO segments and associated water of hydration, with the remaining EO segments in the bulk solution.

MD simulations (to be discussed later) show that in PFOA+PEO complexes several EO segments are in close contact with CF<sub>2</sub> groups. Based on this, among the two composition scenaria considered here, scenario 2 best describes the PFOA + PEO mixed micelles: their shell comprises 1 CF<sub>2</sub> group of each PFOA fluorocarbon chain, carboxylate headgroups, counterions,

and associated water molecules, and a fraction of the PEO polymer. The expressions that describe the PFOA + PEO structure/composition for scenario 1 and the corresponding SANS results are presented in the SI document. Equations for scenario 2 are presented below.

The micelle core radius (b) was obtained from the extended length of a fluorocarbon chain given  $by^{60}$ 

$$l_{f,c}(in \, \text{Å}) = 1.3n_c + 2.04$$
 (3)

where  $n_c$  is the number of carbon atoms in the fluorocarbon tail of the surfactant ( $n_c$  is 6 for PFOA micelle with 1 CF<sub>2</sub> group located in micelle shell and b = 9.84 Å). The micelle core volume  $V_{core}$  (in Å<sup>3</sup>) is calculated from the surfactant association number  $N_{agg}$  and the volume of the PFOA fluorocarbon chain ( $V_{t,PFOA} = [41.6n_c + 42.4] = 292.0$  Å<sup>3</sup>, for  $n_c = 6$ ), using:

$$V_{core} = \frac{4}{3}\pi ab^2 = N_{agg}V_{t,PFOA} \tag{4}$$

where a is the major radius and b is the minor radius of the ellipsoid micelle core. Considering the volume contributions from one CF<sub>2</sub> group, surfactant headgroups, counterions, fraction of PEO homopolymer in the shell, and associated water molecules, the micelle shell volume can be written as:

$$V_{shell} = N_{agg} (V_{CF_2} + V_{COO^-} + (1 - \alpha)V_{NH_4^+} + N_H V_{D_2O}) + n_{EO}(V_{EO}) + n_{EO}N_{H,EO}(V_{D_2O})$$
(5)

where  $V_{CF_2}$ ,  $V_{COO^-}$ ,  $V_{NH_4^+}$ ,  $V_{D_2O}$  and  $V_{EO}$  are the volumes of the CF<sub>2</sub> group, PFOA headgroup, counterion  $NH_4^+$ , D<sub>2</sub>O molecule, and ethylene oxide monomer, respectively,  $\alpha = Z/N_{agg}$  fractional charge on a micelle (Z is the charge on a micelle), N<sub>H</sub> hydration number of a surfactant molecule, n<sub>EO</sub> number of EO segments in the micelle shell, and N<sub>H,EO</sub> water molecules (hydration number)

per EO segment in the micelle shell. On the basis of the reported hydration numbers for  $NH_4^+$  ion<sup>61, 62</sup> and PFO<sup>-</sup> ion<sup>63</sup>, we fixed  $N_H = 12$ . In addition, we fixed  $N_{H,EO} = 4.6$  based on our SANS results of 3% PEO 10000 in D<sub>2</sub>O considering the correlation length model.

The scattering length density of the micelle core is calculated by:

$$\rho_{core} = \frac{N_{agg}b_{CF_3(CF_2)_5}}{V_{core}} \tag{6}$$

where b<sub>i</sub> is the coherent scattering length of molecule i. b<sub>i</sub> values are reported in Table S2.

The scattering length density of the micelle shell is calculated using equation 7, which includes the individual contributions to the scattering from surfactant CF<sub>2</sub> group, hydrophilic headgroups, counterions, ethylene oxide monomers of PEO polymer and associated water molecules.

$$\rho_{shell} = \frac{N_{agg} \left[ b_{CF_2} + b_{COO} + (1 - \alpha) b_{NH_4^+} + N_H b_{D_2O} \right] + n_{EO} \left[ b_{EO} \right] + n_{EO} N_{H,EO} \left[ b_{D_2O} \right]}{V_{shell}}$$
(7)

The scattering length density of the solvent  $\rho_{solvent}$  was calculated using the scattering lengths and concentrations of deuterated water and surfactant. The concentration of PFOA present in the bulk solution was considered equal to its CAC value (12.5 mM) obtained from conductivity.

The main parameters resulting from the fit to the SANS data are the micelle association number  $(N_{agg})$ , charge on a micelle (Z), fraction of PEO homopolymer in the shell, and micelle volume fraction  $(\varphi)$ . The calculation of all parameters obtained from the SANS fits are presented in detail in the SI document. We note that the number of parameters that are really "free" in fitting the SANS data for PEO+PFOA mixed micelle are very few: axial ratio of the micelle core, shell thickness, charge on the micelle, source background, correlation length, and Lorentzian scale. Some parameters are known, such as solvent scattering length density  $(\rho_{solvent})$ , temperature,

dielectric constant of solvent. Other parameters we fixed to very reasonable values, for example, we set the minor radius of the micelle core equal to the extended length of the surfactant alkyl chain, we considered uniform shell thickness (i.e., ratio of thickness of shell at pole to that at equator = 1), we considered the micelle core to consist of only PFOA fluorocarbon chains and hence the micelle core scattering length density ( $\rho_{core}$ ) is set to  $\rho_{CF3(CF2)6}$ . We assumed Gaussian nature of the PEO chains present in solution (i.e., Lorentzian exponent = 2). We fixed the Porod scale (A) = 0, since the scattering behavior at low q values does not show clustering (no decrease in the scattering intensity at low q values). Other important parameters, such as micelle association number ( $N_{agg}$ ), fractional charge on a micelle ( $\alpha = Z/N_{agg}$ ), and average number of ethylene oxide monomers of PEO homopolymer in the micelle shell ( $n_{EO}$ ), are calculated from the parameters obtained from fitting SANS intensity data.

The SANS form and structure factors used in this study are similar to those previously used in the literature.<sup>6</sup> We have used the correlation length model to fit SANS data from PEO in D<sub>2</sub>O, as was previously used.<sup>6</sup> We utilized core-shell ellipsoid form factor with Hayter RMSA structure factor to describe PFOA micelles with a fraction of PEO present in the micelle shell, and capture the scattering in the intermediate and high q range. Furthermore, we incorporated to the overall scattering intensity the correlation length model which captures the scattering at low-q values originating from polymers in aqueous solution. We note that, for the 110 mM PFOA in D<sub>2</sub>O sample, the scattering intensity data points in the low-q region exhibit relatively large error bars and an upturn in the intensity, which is common in scattering from surfactant solutions, and is typically attributed to scattering from tiny air bubbles that are stabilized by surfactant. Such an upturn is not observed in samples containing 3% PEO where the overall intensity is a factor 10 higher, resulting in much higher signal-to-noise ratio.

# Molecular Dynamics (MD) Simulations

All MD simulations were conducted using a non-polarizable version of Atomistic Polarizable Potentials for Liquids, Electrolytes and Polymers (APPLE&P),<sup>64</sup> which has been previously used in the investigation of perfluorinated surfactant self-assembly in water in the presence of ethanol or urea additives.<sup>49, 53</sup> Studied systems contained 32 PFOA surfactant+counterion pairs and 4032 H<sub>2</sub>O molecules. This concentration (about 390 mM) is well above the CMC, as shown in previous simulations,<sup>49, 53</sup> PFOA molecules form one large micelle with association number N<sub>agg</sub>=32. To investigate the influence of PEO on the micelle structure, we considered a series of systems containing 1, 2, 3 or 4 PEO chains with degree of polymerization 50 (MW=2202 g/mol), which correspond to 2.5, 5.0, 7.5 and 10 wt% PEO in solution, respectively. Note, that direct simulations of the polymer molecular weights used in experiments would be very challenging. Hence, we simulated shorter chains with MW=2200 (compared to MW=10000 used in experiments). Simulations with four PEO chains correspond to having a similar number of EO segments per micelle as in experiments.

Initially, all molecules were randomly placed in a simulation cell with reduced density, and the system was condensed to approximately correct density. Then, each system was equilibrated for 5 ns in the NPT ensemble using the Nose-Hoover thermostat and barostat<sup>65</sup> to establish equilibrium density, as well as to allow self-assembly and equilibration of PFOA and polymer chain mixed micelle. Production runs were over 30 ns, which is sufficient for PFO<sup>-</sup> surfactants to move around the micelle, therefore allowing sample fluctuations in micelle shape and conformations of PEO chains. A 15 Å cutoff distance was used for the calculation of van der

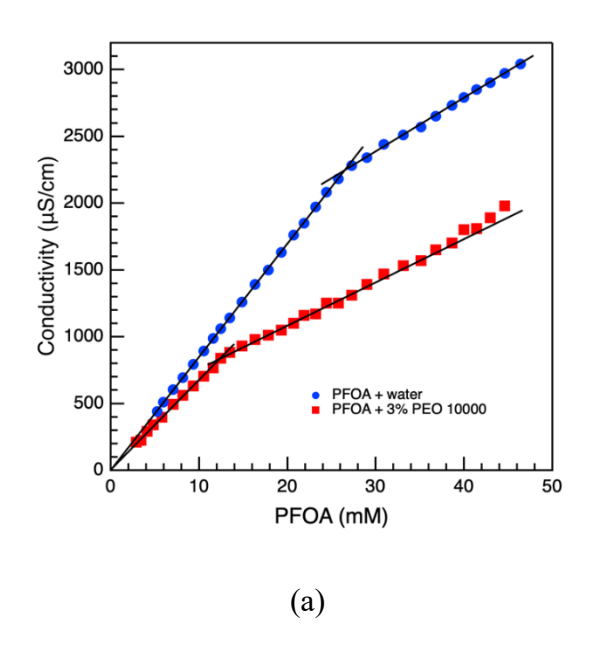
Waals potentials and the real part of Ewald summation for electrostatics interactions.<sup>66</sup> The SHAKE algorithm has been applied to constrain all chemical bonds.<sup>67</sup>

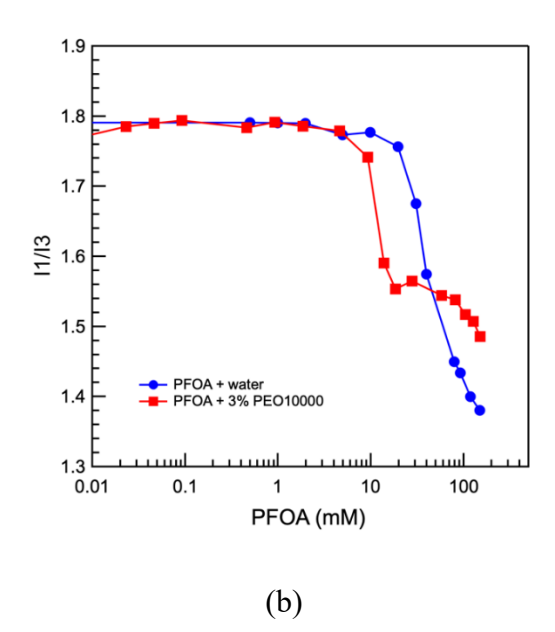
## RESULTS AND DISCUSSION

In what follows, we present experimental data and molecular scale correlations obtained from MD simulations for aqueous PFOA+PEO systems, followed by the discussion of self-assembly and interplay of interactions obtained from this complementary experiment/simulation analysis.

# Critical aggregation concentration

In order to understand the association between PFOA and PEO in the investigated concentration range, and to obtain critical concentrations required for SANS analysis, we measured conductivity, pyrene fluorescence, surface tension, and viscosity for aqueous PFOA+PEO systems as shown in Figure 1. The critical aggregation concentration (CAC) of PFOA obtained from conductivity is  $12.5 \pm 0.5$  mM, and from fluorescence and surface tension is  $10 \pm 0.7$  mM.





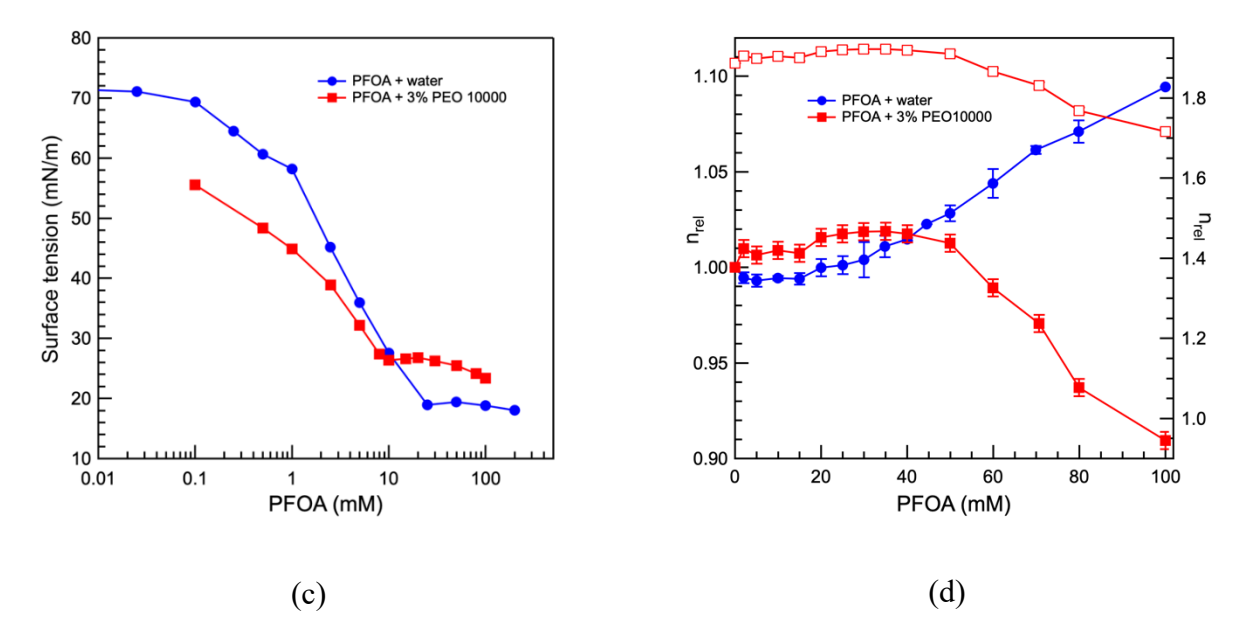


Figure 1. (a) Conductivity (21 °C), (b) pyrene fluorescence I1/I3 ratio (22 °C), (c) surface tension (20 °C), and (d) relative viscosity (20 °C) of aqueous PFOA+3% PEO 10000 solutions plotted as a function of surfactant concentration. In the conductivity and surface tension plots, error bars are smaller than the size of the symbols and, hence, not visible. The relative viscosities ( $\eta_{rel} = \eta/\eta_0$ ) for PFOA+PEO solutions are calculated considering  $\eta_0$  as the viscosity of plain water (open symbols) and as the viscosity of aqueous PEO solution (closed symbols).

The CAC value indicates that we expect association between PFOA and PEO to occur in the concentration range where we operate. The CAC of PFOA in 3% PEO 10000 solution is lower than the CMC in plain water (26.5 mM).<sup>46</sup> The CAC value agrees well with the CAC of perfluorooctanoate salts in aqueous PEO solutions reported in the literature.<sup>40, 43</sup> The CAC values of cesium perfluorooctanoate (CsPFO) (CMC = 23.4 mM) decreased as the PEO MW increased, and reached an almost constant value of 9 mM for MW > 4600.<sup>40</sup> The CAC values for SDS (CMC = 8.4 mM) also decreased with PEO MW and became 4.2 mM for MW > 4600.<sup>44</sup>

The degree of counterion dissociation ( $\alpha$ ) of PEO-bound PFOA micelles estimated from the ratios of the slopes of the straight lines fitted to conductivity data is 0.53, which is slightly higher

than the  $\alpha$ =0.47 value of polymer-free PFOA micelles. In agreement with this finding,  $\alpha$  values of PEO-bound perfluoroalkyl carboxylates micelles are greater than  $\alpha$  of the corresponding free micelles. For SDS+PEO complexes  $\alpha$ =0.56, while for free SDS micelles  $\alpha$ =0.38. The polymer to water than in solution (CAC < CMC) and can relate to the greater counterion dissociation in polymer-bound micelles compared to free surfactant micelles. The polymer is diluting the headgroup charges, hence less of a need for counterion condensation, and a bigger fraction of counterions are free to come and go in the solution, yielding a favorable entropic contribution to the Gibbs free energy of micellization of surfactant molecules on polymer chain.

Information on the microenvironment of PFOA+PEO mixed micelles is obtained from pyrene fluorescence I<sub>1</sub>/I<sub>3</sub> data. For the PFOA + 3% PEO 10000 system, I<sub>1</sub>/I<sub>3</sub> remains constant at low surfactant concentrations since the surfactant is not associated and the pyrene molecules are in the aqueous bulk solution. I<sub>1</sub>/I<sub>3</sub> starts to decrease above 10 mM PFOA which corresponds to the CAC, above which, PFOA forms complexes with PEO. The decrease in the I<sub>1</sub>/I<sub>3</sub> ratio can be interpreted as pyrene moving from bulk solution into the hydrophobic domain of PFOA+PEO micelles. The I<sub>1</sub>/I<sub>3</sub> ratio remains approximately constant in the 18 – 80 mM PFOA range and decreases gradually above 80 mM. This constant I<sub>1</sub>/I<sub>3</sub> at 18 – 80 mM is attributed to a complete pyrene solubilization into the PFOA+PEO complexes.<sup>68</sup> Similar I<sub>1</sub>/I<sub>3</sub> trend was observed for aqueous solutions of lithium perfluorononanoate (LiPFN) and poly(vinylpyrrolidone) (PVP).<sup>68</sup>

The surface tension of PFOA aqueous solution (Figure 1c) starts a plateau region at 25 mM, which corresponds to the CMC.<sup>46</sup> The surface tension trends are more complex in surfactant + polymer systems at fixed polymer concentration and increasing surfactant concentration.<sup>13, 69</sup> In

general, the surface tension decreases and reaches a first plateau region at the CAC. $^{43, 69}$  Upon further increase in surfactant concentration, the surface tension decreases again above PSP, and reaches a second plateau region which corresponds to the concentration at which free surfactant micelles form in the aqueous solution. $^{43, 69}$  In the case of PFOA + 3% PEO 10000, the surface tension reached the first plateau region at 10 mM which corresponds to the CAC. This CAC value matches that obtained from conductivity. With increasing PFOA concentration, the surface tension gradually decreased, however, a second plateau region was not observed at the studied concentration region (0–100 mM PFOA). This suggests that, for the PFOA + 3% PEO 10000 system, formation of free PFOA micelles will not happen even at 100 mM PFOA, and PFOA will bind to PEO molecules throughout the 10-100 mM concentration region.

The relative viscosity of PFOA + 3% PEO 10000 aqueous solutions (Figure 1d) increases slightly until 20 mM, remains constant until 50 mM, and decreases above. In general, the relative viscosity of aqueous surfactant solutions increases with an increase in the volume fraction of the solute. The observed decrease in relative viscosity with an increase in surfactant concentration suggests a change in the polymer conformation. For other perfluorooctanoate salt + PEO 8000 (0.5 wt%) systems, the relative viscosity was reported to increase up to the CAC, then decrease, reach a minimum and, at larger surfactant concentrations, increase steeply and monotonically. The viscosity minimum occurred in the concentration region of an endothermic maximum observed in ITC curves, which was ascribed to the initial coiling of the polymer around a small surfactant cluster leading to a strained high-energy conformation, which then evolves to a more extended conformation as the cluster bound to the polymer grows with increasing surfactant concentration. An increase in relative viscosity at higher surfactant concentrations was not observed here in the PFOA + 3% PEO 10000 system. This is due to the high PEO concentration

(3 wt%) used in our study, with added PFOA binding to polymer molecules throughout the PFOA concentration range where viscosity was measured.

The above findings prove the binding of PFOA to PEO molecules above CAC=10 mM, however the structure and composition of the formed PFOA+PEO complexes are unknown. To resolve this, we analyze next the structure of PFOA+PEO assemblies in solution. SANS provides direct structural information on the PFOA+PEO complexes, whereas MD simulations provide valuable information on the structure, interactions, and association mechanisms between PFOA and PEO molecules. Results from atomistic MD simulations are considered first.

## PFOA+PEO mixed micelle structure: Insights from MD simulations

PEO is water-soluble but is amphiphilic and, therefore, will experience several competing interactions. PEO forms hydrogen bonds with water and adapts favorable polar conformations containing large fraction of gauche conformers around the C-C bond;<sup>70</sup> polar EO segments can have strong electrostatic interactions with PFOA headgroups and counterions, as well as have hydrophobic interactions with fluorocarbon tails to lower the entropy penalty by reducing the accessible hydrophobic surface to H<sub>2</sub>O.<sup>12, 71</sup> A delicate balance of these competing interactions will define the PEO-PFOA self-assembly in the solution. Initially, our simulations were set up with random distribution of PFOA and PEO chains in solution. However, as the simulation progressed, we observe formation of a PFOA micelle with PEO chain(s) always interacting with the micelle. Figure 2a shows a snapshot of a PFOA micelle in water (no PEO), as well as equilibrated PFOA+PEO mixed micelles with 1, 2 and 4 PEO chains (Figure 2b, c, d). In the

system with 1 PEO chain, we can see that the whole chain is tightly wrapped around the micelle. As the number of PEO chains increases, we see more PEO segments extend into the water phase.

Radial density profiles of F atoms and PEO ether oxygens, O<sub>PEO</sub>, relative to the center of mass of the PFOA micelle are shown in Figure 2e. At r = 0, i.e., the micelle core, we see some reduction of F atom density due to several factors: hard to define density in spherical shells with high curvature and radius smaller than the atom size, as well as high fraction of C atoms and voids contributing in such small volumes. Despite this reduction, there are no water molecules in the core (not shown) and no PEO segments, as can be seen from Figure 2e. Instead, PEO segments are distributed on the surface of the micelle, i.e., the region where the density of F atoms decreases sharply. Similar behavior of PEO has been observed in its interaction with hydrocarbon surfactant micelles, notably SDS, both experimentally<sup>6, 8, 44</sup> and computationaly.<sup>12</sup> MD simulations have indicated that SDS+PEO association is largely driven by a mutual reduction in hydrophobic contact with water of the hydrocarbon tails of SDS and the ethylene units in PEO, leading to release of water molecules from the hydrophobic regions of the polymer and micelle surface, and associated increase in the entropy of water. The propensity of ether oxygens to remain hydrated prevents the solubilization of PEO in the micelle interior.<sup>12</sup>

As the number of PEO chains in the system increases, the PEO density profile peak shifts to longer distances, and higher density of EO segments is observed in the water phase. Therefore, PEO is shielding effectively fluoroalkyl tails from contact with water. Note that, as we showed in previous work,<sup>49</sup> in the system without PEO chains, i.e. only PFOA micelle, a significant portion of F atoms are exposed to water (as can also be seen in Figure 2a) since the headgroups and bound counterions are not sufficient to cover the whole micelle surface. As a result, there is plenty of F-exposed area where PEO segments can efficiently adsorb and interact with the

micelle. Even in the system with 4 PEO chains (which is comparable in total number of EO segments to one longer PEO chain investigated in experiments), most PEO segments can find space to incorporate themselves into the micelle shell.

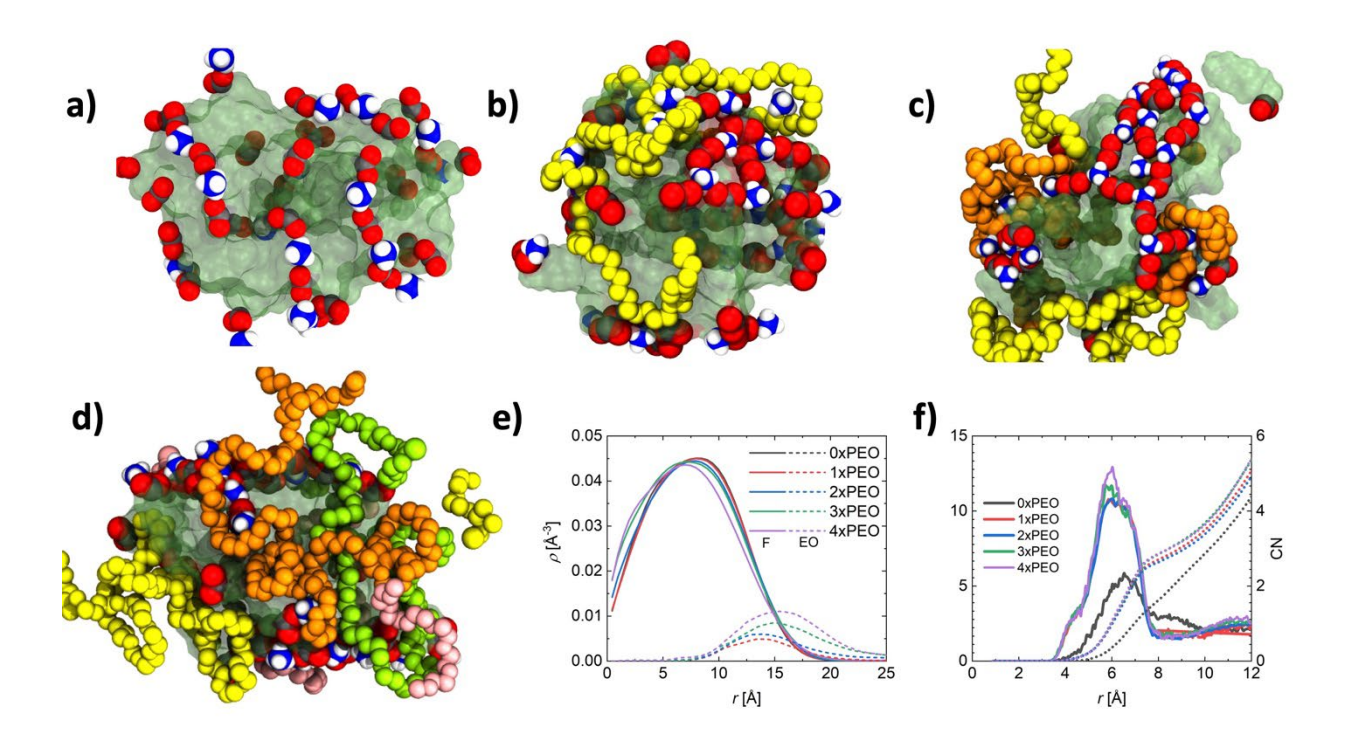


Figure 2. Snapshots of PFOA+PEO mixed micelles in systems with (a) no PEO, (b) one PEO chain, (c) two PEO chains, and (d) four PEO chains. Red atoms: oxygen atoms of PFOA headgroups, blue: nitrogen atoms of ammonium counterion, white: hydrogen atoms of ammonium, translucent green: F atoms of PFOA. PEO chains are shown only with backbone atoms, with each chain having different color (yellow, orange, lime, pink). (e) Number density profiles of F and O<sub>PEO</sub> atoms relative to the center of the micelle. (f) Radial distribution function g(r) of PFOA headgroups (solid lines, left Y axis) and corresponding apparent coordination numbers CN (dashed lines, right Y axis) as a function of distance from the headgroup.

The exposure of PFO<sup>-</sup> fluorocarbon tails to water molecules causes energy and entropy penalty due to hydrophobic interactions. Therefore, the self-assembly of perfluorinated surfactants in water tends to minimize the contact of F atoms with water by distributing ionic headgroups and counterions on the micelle surface. Figure 2a shows that, besides the headgroups, a large fraction of counterions (about 60%) resides at the micelle surface, often interacting with two headgroups.<sup>49</sup> In the absence of PEO chains in the system, the ionic headgroups of the micelle form cation-anion linear clusters and maintain a relatively homogeneous distribution on the micellar surface. Figure 2f shows the radial distribution function (RDF) of C<sub>sp2</sub>-C<sub>sp2</sub> (carbon atoms of headgroup) and the corresponding coordination number (CN). In the system with no PEO chains, a peak around 6.5 Å is observed in the RDF, indicating a higher-than-average probability of finding another headgroup at that distance from the center of PFOA headgroup. The corresponding CN shows about one headgroup within that distance, which is consistent with the configuration depicted in Figure 2a where two headgroups can be "bridged" by ammonium cation. However, as more PEO chains are added to the system, tighter packing of headgroups on the micelle surface is observed. This is further supported by RDFs and CN in Figure 2f where significant increase in the RDF peak can be seen, and the CN exceeds 2.0 within the same coordination shell of 6.5 Å. The location of the RDF peak shifts towards closer distances, indicating a tighter packing of ionic groups on the micelle surface. The influence of PEO chains on the PFOA micelle is consistent with a previous study of PEO with an SDS micelle.<sup>12</sup>

The observed condensation/segregation of PFO<sup>-</sup> headgroups following addition of PEO chains would likely affect the micelle shape. To characterize changes in micelle shape, we have analyzed the gyration tensors of the PFOA micelle, defined as  $S_{kl} = \frac{1}{M} < \sum_{i=1}^{N} m_i k_i l_i >$ , where N is the number of all atoms of PFO<sup>-</sup> molecules comprising the micelle (ammonium counterions

are not included);  $k_i$ ,  $l_i$ , are x, y, z coordinates of atom i relative to the position of the micelle center of mass;  $m_i$  is the atomic mass of atom i; M is the total mass of the micelle; and <> defines averaging over multiple snapshots obtained from simulation trajectories. The calculated  $S_{kl}$  components are reported in Table 1. In the system without PEO chains, the PFOA micelle has slightly oblate shape, with the largest dimension about 40% larger than the smallest. As PEO chains are added in the system, the smallest component,  $S_{xx}$ , remains unchanged, while two other components increase by 50%, indicating an oblate shape of the micelle. Note that, in MD simulation, the micelle association number remains the same and, hence, the reported changes in micelle shape do not take into account possible changes in the micelle association number which can adjust upon addition of PEO (see discussion of SANS data below).

Table 1. Gyration tensor of PFO micelle as a function of PEO content.

System	$S_{xx}$ [Å <sup>2</sup> ]	$S_{yy}$ [Å <sup>2</sup> ]	$S_{zz}[A^2]$	$\sqrt{S_{zz}/S_{xx}}$
No Polymer	31.0	42.9	64.3	1.44
1xPEO <sub>50</sub>	33.0	48.0	70.6	1.46
2xPEO <sub>50</sub>	36.8	51.6	84.1	1.51
3xPEO <sub>50</sub>	36.2	63.4	96.1	1.63
4xPEO <sub>50</sub>	35.9	64.3	96.9	1.64

PFOA+PEO mixed micelle structure: SANS evidence

The MD simulation results discussed above provide valuable information on the arrangement of PFOA and PEO segments within PFOA+PEO mixed micelles, and the shape of the micelles. In what follows we integrate such knowledge of composition and shape into the analysis of SANS data, in order to obtain quantitative information on the size and structure of PFOA+PEO mixed micelles. SANS intensity has been recorded for aqueous 3% PEO 10000 solutions (no surfactant added), aqueous 33 mM or 110 mM PFOA solutions (no polymer added), and aqueous PFOA + 3% PEO10000 solutions at 33 and 110 mM PFOA. In the absence of ionic surfactant, scattering from 3% PEO 10000 does not show any correlation peak (Figure 3). However, upon addition of 33 or 110 mM PFOA a pronounced peak appears, which suggests a polyelectrolyte behavior owing to repulsive interactions between the bound micelles. Note that in the scattering profiles from both 110 mM PFOA (no polymer present) solution and 110 mM PFOA+3% PEO solution, the correlation peak falls at the same Q value, which indicates the same intermicelle distance in both systems. As discussed below in this section, at 110 mM PFOA + 3% PEO 10000, almost all PEO molecules are bound to PFOA micelles (one PFOA micelle per PEO 10000 chain) and the average distance of the polymer molecules in solution obtained is the same as the intermicelle distance. Hence, we can conclude that the peak corresponds to correlation between PEO+PFOA mixed micelles. According to Figure 3, the overall scattering intensity from 33 mM or 110 mM PFOA + 3% PEO 10000 (I<sub>33 mM</sub> PFOA+3% PEO10000 or I<sub>110 mM</sub> PFOA+3% PEO10000) which includes contributions from both surfactants and polymers in solution is very different from the intensity resulting from the algebraic summation of the individual component scattering, i.e., PFOA alone and PEO alone (I<sub>33mM or 110 mM PFOA</sub> + I<sub>3% PEO10000</sub>). This comparison suggests altered polymer conformation or surfactant micelle structure in PFOA+PEO complexes from their original states in water. This is consistent with observations from MD simulations which showed that PEO

chains adjust their conformations to partition at the micelle/water interface. Quantitative information on the structure of PFOA+PEO complexes is obtained by analyzing the scattering profiles of 33 mM + 3% PEO 10000 or 110 mM PFOA + 3% PEO 10000.

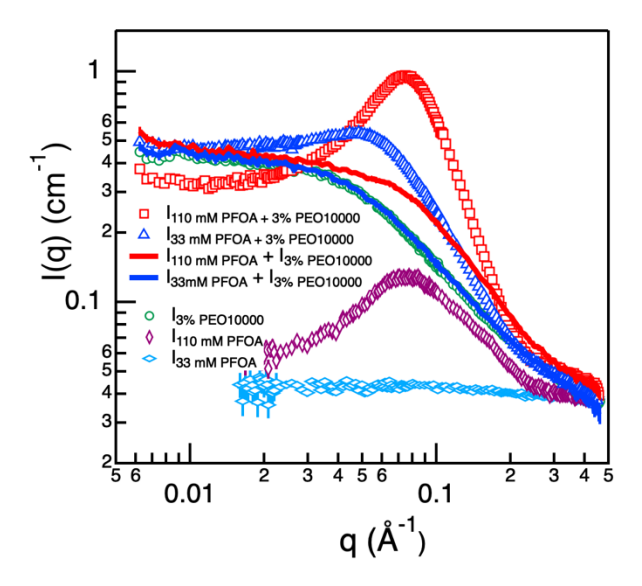


Figure 3. SANS absolute intensity profiles of 33 mM and 110 mM PFOA in 3% PEO10000  $D_2O$  solutions at 22 °C, corrected for  $D_2O$  scattering. The intensities of 110 mM and 33 mM PFOA are added to the intensity of 3% PEO10000 (all three are corrected for  $D_2O$ ) and compared with the original intensities measured for 33 mM and 110 mM PFOA in 3% PEO10000.

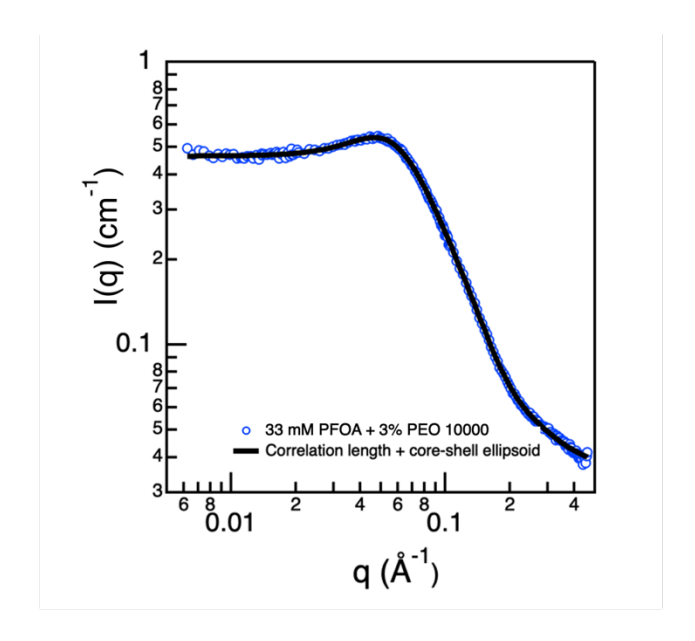
Table 2 summarizes important parameters obtained by fitting 33 mM PFOA + 3% PEO 10000 and 110 mM PFOA + 3% PEO 10000 SANS intensities, corrected for solvent (D<sub>2</sub>O) scattering, using the correlation length + core shell ellipsoid Hayter MSA model, considering one PFOA micelle bound to one PEO chain and scenario 2 (1 CF<sub>2</sub> group of PFOA located in the micelle shell). Also shown are parameters obtained by fitting SANS data of 110 mM PFOA in D<sub>2</sub>O,

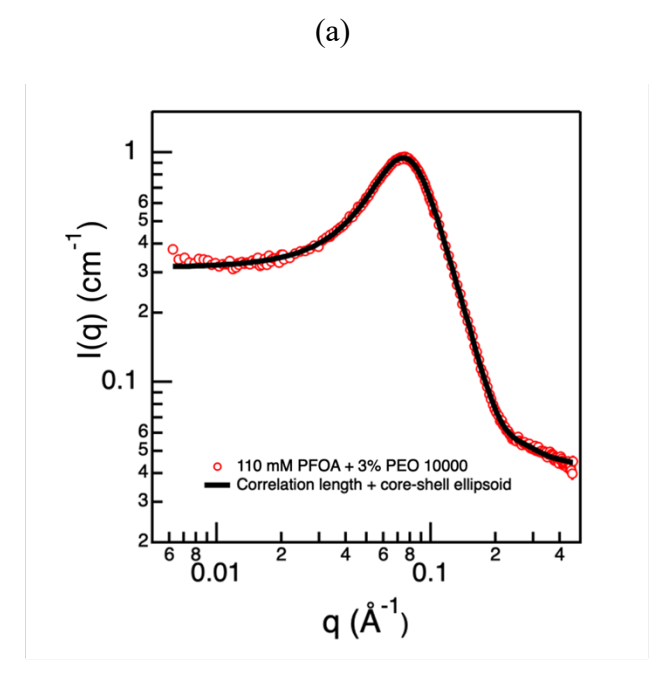
corrected for solvent (D<sub>2</sub>O) scattering, using the core shell ellipsoid Hayter MSA model. Figure 4 shows SANS experimental data and fits to the above models.

Table 2. Parameters obtained by fitting SANS data of 33 mM PFOA + 3% PEO 10000 in  $D_2O$  corrected for solvent  $(D_2O)$  scattering using correlation length + core shell ellipsoid Hayter MSA model and parameters obtained by fitting SANS data of 110 mM PFOA in  $D_2O$  corrected for solvent  $(D_2O)$  scattering using core shell ellipsoid Hayter MSA model.

C <sub>PFOA</sub> (mM)	N <sub>agg</sub>	α	b (Å)	3	δ(Å)	$n_{\rm EO}$	f	$V_{PEO,}$ shell	$V_{\rm D2O,}$ shell	d (Å)	I <sub>peak</sub>	$\chi^2$
With PEO (3 wt%)												
33	40.8	0.23	9.84	2.98	9.42	144	0.63	19.3	71.9	130.9	0.55	1.3
	(±1.0)	$(\pm 0.007)$		$(\pm 0.07)$	(±0.12)	(±4.4)	$(\pm 0.02)$	$(\pm 0.7)$	(±1.8)			
110	33.4	0.36	9.84	2.44	9.72	142	0.62	20.7	71.6	82.7	0.95	1.6
	(±0.6)	$(\pm 0.007)$		$(\pm 0.04)$	$(\pm 0.06)$	(±2.5)	(±0.01)	(±0.4)	(±1.1)			
	No PEO											
110	30.0	0.27	11.14	1.73	4.12	0	0	0	85.0	82.7	0.09	2.5
	(±0.2)	$(\pm 0.004)$		(±0.01)					(±0.8)			

 $C_{PFOA}$  is the PFOA concentration,  $N_{agg}$  micelle association number,  $\alpha$  fractional charge or charge per surfactant molecule in a micelle, b micelle core minor radius,  $\epsilon$  ratio of micelle core major to minor axis,  $\delta$  shell thickness,  $n_{EO}$  average number of ethylene oxide monomers of PEO homopolymer in the micelle shell, f fraction of PEO homopolymer in the micelle shell (ratio of  $n_{EO}$  and total number of ethylene oxide monomers per PEO 10000 homopolymer,  $V_{PEO,shell}$  percentage of micelle shell volume occupied by PEO,  $V_{D2O,shell}$  percentage of micelle shell volume occupied by  $D_2O$ , d inter-micelle distance, and  $I_{peak}$  intensity at the correlation peak maximum.  $\chi^2$  is a statistical parameter that quantifies the differences between the calculated and experimental SANS data set. The uncertainties in the major parameters (shown in parenthesis) are calculated by applying propagation of errors using statistical uncertainties of the fitting parameters.





(b)

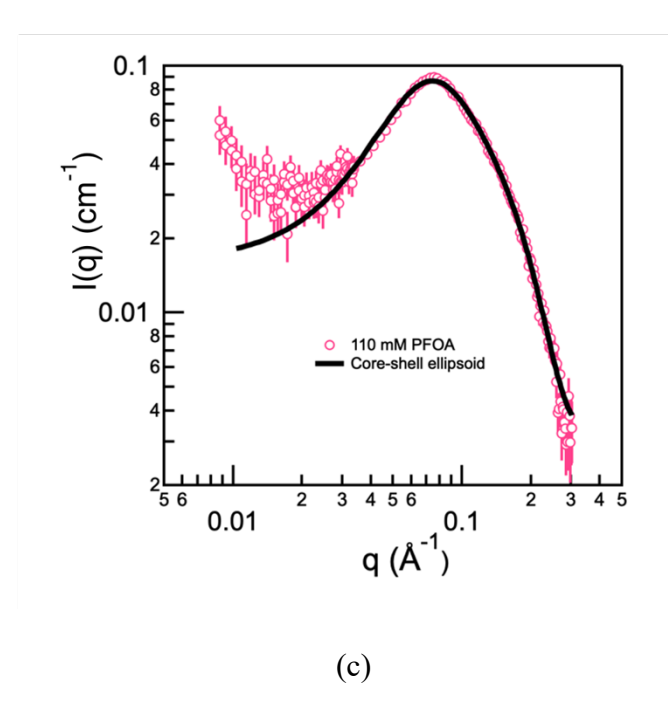


Figure 4. SANS experiment data and fits to the Correlation length + Core shell ellipsoid Hayter MSA model for (a) 33 mM PFOA + 3% PEO 10000 in  $D_2O$  and (b) 110 mM PFOA + 3% PEO 10000 in  $D_2O$ ; SANS experiment data and fits to the core shell ellipsoid Hayter MSA model for (c) 110 mM PFOA in  $D_2O$ . Markers represent SANS absolute intensity profiles and solid line represents model fits to the data.

The physical picture that emerges for a PFOA+PEO mixed micelle formed at the lower PFOA concentration considered here, 33 mM, is that of a core-shell ellipsoid comprising an average of 41 PFOA molecules bound to one PEO 10000 molecule. The micelle core consists of only PFOA alkyl chains, while the micelle shell consists of PFOA CF<sub>2</sub> groups (4 vol%), headgroups and counterions (5 vol%), EO segments of the PEO chain (19 vol%), and hydration water (72 vol%). The core minor radius is 9.8 Å, the ratio of core major to minor axis is 3.0, the shell thickness is 9.4 Å, and the fractional charge on the micelle is 0.23. At 33 mM PFOA, 144 EO segments reside in the PFOA micelle shell, which constitute 63% of the PEO 10000 chain.

The PFOA+PEO mixed micelles formed at the higher PFOA concentration, 110 mM, are coreshell ellipsoids comprising an average of 33 PFOA molecules bound to one PEO molecule, which is 18% less compared to mixed micelles formed at 33 mM PFOA. Upon a PFOA concentration increase from 33 to 110 mM, ε decreased by 18%, i.e., the micelles became less elongated, while the fractional charge increased by 56%. The compositions of the micelle core and micelle shell at 110 mM PFOA are the same as in the 33 mM case; also the fraction of the PEO chain residing in the micelle shell.

Both scenario 2 (the results of which are discussed above) and scenario 1 (no CF<sub>2</sub> groups in the micelle shell; results presented in the SI document) show the PEO-bound PFOA micelles to be more elongated than free PFOA micelles, in agreement with MD simulations, and the key features/conclusions remain unchanged. Scenario 1 gives slightly higher N<sub>agg</sub> and slightly lower n<sub>EO</sub> and f values compared to scenario 2, but the equivalent spherical micelle radius (R<sub>eq</sub> = 23.5 Å) is the same for both scenaria. Both SANS fits (Table 2) and MD analysis (Table 1) conclude on an ellipsoidal shape for the PFOA+PEO mixed micelles; SANS suggests prolate ellipsoids while MD prolate ellipsoids, possibly due to the different association numbers and PEO molecular weight in the experiments and modeling.

In order to estimate the fraction of PEO 10000 molecules which are not associated with PFOA micelles in the bulk aqueous solution, we first obtained the radius of gyration ( $R_g = \sqrt{2} \xi$ ) value from the correlation length ( $\xi$ ). For 33 mM PFOA + 3% PEO 10000, the  $\xi$  value obtained from fitting equation 1 to SANS intensity profile is  $\xi = 16.0$  Å and  $R_g = 22.6$  Å, which is the same as the radius of gyration of 3% PEO 10000 in plain water ( $R_g = 22.4$  Å). For 110 mM PFOA + 3% PEO 10000,  $\xi = 12.3$  Å and  $R_g = 17.4$  Å, which is 28% lower than the radius of gyration of 3% PEO 10000 in plain water. From the micellized PFOA concentration ( $C_{PFOA} - CAC$ ) and the

micelle association number, we can estimate the number of micelles in solution. Taking one PEO chain per PFOA micelle, we estimate the number of PEO molecules not associated with PFOA micelles in solution. At 33 mM PFOA + 3% PEO 10000, 19% of PEO molecules are bound to PFOA micelles, while the remaining 81% are separate from PFOA micelles, in the bulk aqueous solution. At 110 mM PFOA + 3% PEO 10000, however, almost all PEO molecules are bound to PFOA micelles. From R<sub>g</sub> we calculate the volume of a sphere with R<sub>g</sub> radius which corresponds to the hydrated volume of a PEO molecule not associated with PFOA micelles. From this hydrated volume and the number of PEO molecules left outside PFOA micelles, we estimate the volume fraction of PEO molecules left outside PFOA micelles in solution,  $\emptyset_{poly}$ . From the volume of PEO-bound PFOA micelles, volume of EO segments of micelle-bound PEO chain residing in bulk solution, and number of micelles in solution, we estimate the volume fraction of PFOA+PEO complexes in solution,  $\emptyset_{complex}$ . The volume fraction of the solute (polymer + micelles) in water is given by  $\emptyset = \emptyset_{poly} + \emptyset_{complex}$ . At 33 mM PFOA + 3% PEO 10000,  $\emptyset =$  $\emptyset_{poly} + \emptyset_{complex} = 0.0977$ , while the volume fraction of the "dry" (not hydrated) mass of surfactant and polymer present in water is  $\phi_{dry} = 0.0388$ . At 110 mM PFOA + 3% PEO 10000,  $\emptyset = \emptyset_{poly} + \emptyset_{complex} = 0.1298$ , and  $\emptyset_{dry} = 0.0564$ . With the increase in PFOA concentration from 33 to 110 mM, the volume fraction of the "dry" mass in water  $\emptyset_{dry}$  increased by 45% and the hydrated volume fraction of the solute (polymer + micelles) in water increased by 33%. It should be noted that throughout the calculations we assumed the average number of water molecules hydrating an EO segment in PFOA+PEO complexes to be the same as the number of water molecules hydrating an EO segment in 3% PEO 10000 in water in the absence of surfactant. While some EO segments replace water at the surface of the micelle core, the micelle shell is highly hydrated and EO segments can still make H-bonds with water.

To validate the outcome from SANS fits that PFOA+PEO mixed micelles (i.e., PFOA micelle bound to a single PEO chain) coexist with PEO molecules free in the aqueous solution, we estimated the average distance of the polymer molecules in solution obtained as  $(yN_A/M_w)^{-1/3}$  = 82.1 Å (N<sub>A</sub> is the Avogadro number, M<sub>w</sub> polymer molecular weight, y is the concentration of polymer in g/cm<sup>3</sup> units). <sup>11</sup> At 110 mM PFOA + 3% PEO 10000, almost all of PEO molecules are bound to PFOA micelles and the average distance of the polymer molecules in solution obtained is the same as the intermicelle distance 82.7 Å. This indicates that the distance between two adjacent micelles is the same as the average distance of the adjacent polymer molecules, which means one PFOA micelle per PEO 10000 chain. At 33 mM PFOA + 3% PEO 10000, 19% of PEO molecules are bound to PFOA micelles, while the remaining 81% of PEO molecules are separate from PFOA micelles, in the bulk aqueous solution. In the case of 33 mM PFOA + 3% PEO 10000, the average distance of the polymer molecules bound to PFOA micelles in solution obtained as  $(yN_A/M_w)^{-1/3} = 142.7$  Å (y is the concentration of polymer bound to PFOA micelles in g/cm<sup>3</sup> units), is close to the intermicelle distance 130.9 Å, indicating that our assumption is valid.

Compared to free PFOA micelles ( $\varepsilon$  = 1.7), PEO-bound PFOA micelles ( $\varepsilon$  = 2.4) are elongated by 41%, which is qualitatively consistent with gyration tensor changes obtained by MD simulations. The association number of PEO-bound PFOA micelles at 110 mM PFOA is 10% greater compared than that of free PFOA micelles at the same PFOA concentration. The fractional charge of PEO-bound PFOA micelles ( $\alpha$  = 0.36) at 110 mM PFOA is also greater by 33% compared to that of free PFOA micelles ( $\alpha$  = 0.27). This is in agreement with the higher degree of counterion dissociation  $\alpha$  values obtained from conductivity for PEO-bound PFOA micelles compared to free PFOA micelles. SANS analysis gives the percentage of the micelle

(core+shell) volume occupied by water in PFOA+PEO complexes to be 59%, while in free PFOA micelles it is 48%. The lower water content in free PFOA micelles suggests a more hydrophobic environment. This is consistent with pyrene fluorescence results: I<sub>1</sub>/I<sub>3</sub> ratios of PFOA+PEO complexes are greater than I<sub>1</sub>/I<sub>3</sub> ratios of free PFOA micelles (Figure 1b).

We compare now the size and shape of fluorocarbon surfactant PFOA+PEO mixed micelles to that of hydrocarbon surfactant SDS+PEO mixed micelles. On the basis of the SANS and MD analysis presented here, PEO-bound PFOA micelles are more elongated and slightly bigger in association number ( $N_{agg}$  = 33.4,  $\epsilon$  = 2.4) compared to free PFOA micelles ( $N_{agg}$  = 30,  $\epsilon$  = 1.7) at the same surfactant concentration (110 mM). However, such elongation is not observed in PEObound SDS micelles compared to free SDS micelles. A SANS study on SDS + 0.5 wt% PEO 90000 in water has reported that, at 30 mM SDS, the size and shape of PEO-bound SDS micelles  $(N_{agg} = 79, b = 16.7 \text{ Å}, \epsilon = 1.4)$  are similar to those of free SDS micelles  $(N_{agg} = 76, b = 16.7 \text{ Å}, \epsilon = 1.4)$ = 1.4).6 In the SDS + PEO 90000 system, the molecular weight of the PEO bound per micelle is found 15,000,6 and in SDS + PEO 135000 complexes formed at polymer saturation, the PEO MW per micelle is 13,500.8 Whereas in both of these SDS + PEO systems the PEO MW is much higher than the one we use in this study, the PEO part (MW) per SDS+PEO mixed micelle is consistent with the PEO MW per micelle for our PFOA + PEO 10000 mixed micelles. Key properties of polymer-free PFOA and SDS micelles and of PFOA+PEO and SDS+PEO mixed micelles for are presented in Table 3.

Table 3. Comparison between properties of PFOA (110 mM) and SDS (30 mM) micelles in  $D_2O$ , and properties of mixed micelles 110 mM PFOA + 3 wt% PEO 10000 and 30 mM SDS + 0.5 wt% PEO 90000 in  $D_2O$ . Data for SDS systems are from reference.<sup>6</sup>

	CAC (mM)	CMC (mM)	$N_{agg}$	α	b (Å)	3
PFOA micelles		26.5	30	0.27	11.14	1.73
SDS micelles		7.8	76	0.14	16.7	1.4
PFOA+PEO mixed micelles	1.5		33.4	0.36	9.84	2.44
SDS+PEO mixed micelles	4.2 a		79.4	0.08	16.7	1.4

<sup>&</sup>lt;sup>a</sup> from Ref<sup>44</sup>

## **CONCLUSIONS**

This study provides fundamental insights on association of fluorinated surfactants with polymers in aqueous solution, with an aim to support the design of polymer-based PFAS-adsorbent materials. To this end, the formation and structure of complexes between perfluorooctanoic acid ammonium salt (PFOA) and poly(ethylene oxide) (PEO) (MW=10,000) are obtained from analysis of complementary experimental measurements and atomistic MD simulations.

PFOA binds to PEO at a CAC of 10 mM which is lower than its CMC in water (26.5 mM). The PFOA+PEO mixed micelles are ellipsoid in shape and comprise 33 PFOA molecules (at 110 mM) bound to one PEO 10000 molecule. The PFOA+PEO mixed micelles have 10% higher association number and are 40% more elongated compared to polymer-free PFOA micelles at the same PFOA concentration (110 mM). In agreement with these results from SANS, gyration tensor changes observed in MD simulations also reveal elongated PFOA+PEO mixed micelles. PFOA+PEO complexes offer a less hydrophobic environment than free PFOA micelles according to pyrene fluorescence results and the percentage of the micelle volume occupied by water in PFOA+PEO complexes (59%) or free PFOA micelles (48%) obtained from SANS. The PFOA+PEO mixed micelle composition remained the same at 33 and 110 mM PFOA, but the association number decreased, and the micelles became less elongated when the PFOA concentration increased from 33 to 110 mM. At both 33 and 110 mM, 62% of a PEO 10000 chain reside in the PFOA micelle shell, and the remaining segments of this PEO molecule are tangling out in the solution. At 33 mM PFOA + 3% PEO 10000 aqueous solution, 81% of PEO molecules are not associated at all with PFOA micelles, while at 110 mM PFOA + 3% PEO 10000, almost all PEO molecules are bound to PFOA micelles.

PFAS surfactant binding to PEO is not due to any favorable enthalpic interactions involving fluorocarbon. This has practical implications, as the use of fluorinated functionalities in polymer materials that are designed to bind PFAS <sup>72, 73</sup> has raised concerns due to the potential release into the environment of additional PFAS compounds associated with said materials. PEO, on the other hand, is a rather innocuous and low-cost polymer. PEO binding to PFAS surfactants is facilitated by interactions at the micelle surface. In polymer-free PFOA micelles, a significant portion of F atoms are exposed to water. Both MD and SANS results have shown that PEO chains adjust their conformations to effectively partition on the micelle surface where they shield fluorocarbon from contact with water. MD simulations have shown that PEO chains do not penetrate into the PFOA micelle interior. In the PFOA+PEO mixed micelles, a tighter packing of ionic headgroups on the micelle surface is observed compared to relatively homogeneous distribution of headgroups in polymer-free PFOA micelles. SANS and conductivity results have shown that the degree of counterion dissociation (α) of PEO-bound PFOA micelles is greater than that of free PFOA micelles.

This is the first study to probe the structure of polymers bound to fluorinated surfactants. Further, this is one of very few studies using MD to probe surfactant micelle+polymer interactions. Knowledge of fluorinated surfactant + polymer association in aqueous solutions supports the molecular design of adsorbent materials for selective PFAS sequestration from aqueous media. This study provides valuable information on the interactions and conformation at the atomistic/molecular level of ionic surfactants binding to water-soluble polymers, which are important in achieving product performance of aqueous surfactant- and polymer-based formulations. MD simulations allow for exploration of polymer relative hydrophilicity/hydrophobicity, and predictions on how different polymers will interact with surfactants.

**Supporting Information**: Additional details on experimental techniques and SANS data analysis.

Acknowledgements: This research was funded by the U.S. National Science Foundation (NSF), grant numbers CBET-1930959 and CBET-1930935. We acknowledge the support of the National Institute of Standards and Technology (NIST), U.S. Department of Commerce, in providing the neutron research facilities used in this work. Access to the CHRNS 30m Small-angle neutron scattering instrument was provided by the Center for High Resolution Neutron Scattering (CHRNS), a partnership between NIST and NSF under Agreement No. DMR-1508249. We thank Dr. Yimin Mao at NIST for valuable assistance with the SANS data acquisition. We thank Honeywell Buffalo Research Labs (Greg Smith and Roy Robinson) for providing access to a surface tension instrument.

## **REFERENCES**

- 1. Tsianou, M.; Alexandridis, P., Surfactant polymer interactions. *Surfactant Science Series* **2005**, *124*, 657-708.
- 2. Holmberg, K.; Jönsson, B.; Kronberg, B.; Lindman, B., Surfactants and Polymers in Aqueous Solution, 2nd ed. 2003.
- 3. Sharipova, A. A.; Aidarova, S. B.; Mutaliyeva, B. Z.; Babayev, A. A.; Issakhov, M.; Issayeva, A. B.; Madybekova, G. M.; Grigoriev, D. O.; Miller, R., The use of polymer and surfactants for the microencapsulation and emulsion stabilization. *Colloids and Interfaces* **2017**, *1* (1), 3.
- 4. Bureiko, A.; Trybala, A.; Kovalchuk, N.; Starov, V., Current applications of foams formed from mixed surfactant–polymer solutions. *Advances in Colloid and Interface Science* **2015**, *222*, 670-677.
- 5. Somasundaran, P.; Chakraborty, S.; Qiang, Q.; Deo, P.; Wang, J.; Zhang, R., Surfactants, polymers and their nanoparticles for personal care applications. *Journal of Cosmetic Science* **2004**, *55*, S1-S17.
- 6. Fajalia, A. I.; Tsianou, M., Charging and uncharging a neutral polymer in solution: A small-angle neutron scattering investigation. *Journal of Physical Chemistry B* **2014**, *118* (36), 10725-10739.
- 7. Martínez Narváez, C. D. V.; Mazur, T.; Sharma, V., Dynamics and extensional rheology of polymer–surfactant association complexes. *Soft Matter* **2021**, *17* (25), 6116-6126.
- 8. Cabane, B.; Duplessix, R., Neutron scattering study of water-soluble polymers adsorbed on surfactant micelles. *Colloids and Surfaces* **1985**, *13*, 19-33.

- 9. Chari, K.; Kowalczyk, J.; Lal, J., Conformation of poly(ethylene oxide) in polymer–surfactant aggregates. *Journal of Physical Chemistry B* **2004**, *108* (9), 2857-2861.
- 10. Mears, S. J.; Cosgrove, T.; Obey, T.; Thompson, L.; Howell, I., Dynamic light scattering and small-angle neutron scattering studies on the poly(ethylene oxide)/sodium dodecyl sulfate/polystyrene latex system. *Langmuir* **1998**, *14* (18), 4997-5003.
- 11. Lin, M.; Sinha, S.; Chari, K., Polymer-surfactant assemblies in water. A SANS study. *Le Journal de Physique IV* **1993**, *3* (C8), C8-153-C8-156.
- 12. Shang, B. Z.; Wang, Z.; Larson, R. G., Molecular dynamics simulation of interactions between a sodium dodecyl sulfate micelle and a poly(ethylene oxide) polymer. *Journal of Physical Chemistry B* **2008**, *112* (10), 2888-2900.
- 13. Kancharla, S.; Zoyhofski, N. A.; Bufalini, L.; Chatelais, B. F.; Alexandridis, P., Association between nonionic amphiphilic polymer and ionic surfactant in aqueous solutions: effect of polymer hydrophobicity and micellization. *Polymers* **2020**, *12* (8), 1831.
- 14. Tam, K. C.; Wyn-Jones, E., Insights on polymer surfactant complex structures during the binding of surfactants to polymers as measured by equilibrium and structural techniques.

  Chemical Society Reviews 2006, 35 (8), 693-709.
- 15. Kancharla, S.; Bedrov, D.; Tsianou, M.; Alexandridis, P., Structure and composition of mixed micelles formed by nonionic block copolymers and ionic surfactants in water determined by small-angle neutron scattering with contrast variation. *Journal of Colloid and Interface Science* **2022**, *609*, 456-468.
- 16. Lele, B. J.; Tilton, R. D., Control of the colloidal depletion force in nonionic polymer solutions by complexation with anionic surfactants. *Journal of Colloid and Interface Science* **2019**, *553*, 436-450.

- 17. Patel, D.; Ray, D.; Tiwari, S.; Kuperkar, K.; Aswal, V. K.; Bahadur, P., SDS triggered transformation of highly hydrophobic Pluronics® nanoaggregate into polymer-rich and surfactant-rich mixed micelles. *Journal of Molecular Liquids* **2022**, *345*, 117812.
- 18. Krafft, M. P.; Riess, J. G., Selected physicochemical aspects of poly- and perfluoroalkylated substances relevant to performance, environment and sustainability-part one. *Chemosphere* **2015**, *129*, 4-19.
- 19. Kissa, E., *Fluorinated Surfactants and Repellents, 2nd Edition*. Marcel Dekker, Incorporated: New York, 2001; Vol. 97, p 1-615.
- 20. Kancharla, S.; Alexandridis, P.; Tsianou, M., Sequestration of poly- and perfluoroalkyl substances (PFAS) by adsorption: surfactant and surface aspects. *Current Opinion in Colloid & Interface Science* **2022**, *58*, 101571.
- 21. KEMI (Swedish Chemicals Agency), Occurrence and use of highly fluorinated substances and alternatives. <a href="https://www.kemi.se/en/global/rapporter/2015/report-7-15-occurrence-and-use-of-highly-fluorinated-substances-and-alternatives.pdf">https://www.kemi.se/en/global/rapporter/2015/report-7-15-occurrence-and-use-of-highly-fluorinated-substances-and-alternatives.pdf</a>.
- 22. Kissa, E., *Fluorinated Surfactants: Synthesis, Properties, Applications*. M. Dekker: New York, 1994; Vol. 50.
- 23. Buck, R. C.; Murphy, P. M.; Pabon, M., Chemistry, properties, and uses of commercial fluorinated surfactants. In *Polyfluorinated Chemicals and Transformation Products*, Knepper, T. P.; Lange, F. T., Eds. Springer Berlin Heidelberg: Berlin, Heidelberg, 2012; pp 1-24.
- 24. Moody, C. A.; Field, J. A., Perfluorinated surfactants and the environmental implications of their use in fire-fighting foams. *Environmental Science and Technology* **2000**, *34* (18), 3864-3870.

- 25. Krafft, M. P.; Riess, J. G., Therapeutic oxygen delivery by perfluorocarbon-based colloids. *Advances in Colloid and Interface Science* **2021**, *294*, 102407.
- 26. Xiao, F., Emerging poly- and perfluoroalkyl substances in the aquatic environment: A review of current literature. *Water Research* **2017**, *124*, 482-495.
- 27. Buck, R. C.; Franklin, J.; Berger, U.; Conder, J. M.; Cousins, I. T.; de Voogt, P.; Jensen, A. A.; Kannan, K.; Mabury, S. A.; van Leeuwen, S. P. J., Perfluoroalkyl and polyfluoroalkyl substances in the environment: Terminology, classification, and origins.

  Integrated Environmental Assessment and Management 2011, 7 (4), 513-541.
- 28. Prevedouros, K.; Cousins, I. T.; Buck, R. C.; Korzeniowski, S. H., Sources, fate and transport of perfluorocarboxylates. *Environmental Science and Technology* **2006**, *40* (1), 32-44.
- 29. Brase, R. A.; Mullin, E. J.; Spink, D. C., Legacy and emerging per- and polyfluoroalkyl substances: analytical techniques, environmental fate, and health effects. *International Journal of Molecular Sciences* **2021**, *22* (3), 995.
- 30. Alves, A. V.; Tsianou, M.; Alexandridis, P., Fluorinated surfactant adsorption on mineral surfaces: implications for PFAS fate and transport in the environment. *Surfaces* **2020**, *3* (4), 516-566.
- 31. Domingo, J. L.; Nadal, M., Human exposure to per- and polyfluoroalkyl substances (PFAS) through drinking water: A review of the recent scientific literature. *Environmental Research* **2019**, *177*, 108648.
- 32. Sunderland, E. M.; Hu, X. C.; Dassuncao, C.; Tokranov, A. K.; Wagner, C. C.; Allen, J. G., A review of the pathways of human exposure to poly- and perfluoroalkyl substances (PFASs) and present understanding of health effects. *Journal of Exposure Science & Environmental Epidemiology* **2019**, *29* (2), 131-147.

- 33. Fenton, S. E.; Ducatman, A.; Boobis, A.; DeWitt, J. C.; Lau, C.; Ng, C.; Smith, J. S.; Roberts, S. M., Per- and polyfluoroalkyl substance toxicity and human health review: current state of knowledge and strategies for informing future research. *Environmental Toxicology and Chemistry* **2021**, *40* (3), 606-630.
- 34. Du, Z.; Deng, S.; Bei, Y.; Huang, Q.; Wang, B.; Huang, J.; Yu, G., Adsorption behavior and mechanism of perfluorinated compounds on various adsorbents-A review. *Journal of Hazardous Materials* **2014**, *274*, 443-454.
- 35. Zhang, D.; Zhang, W.; Liang, Y., Adsorption of perfluoroalkyl and polyfluoroalkyl substances (PFASs) from aqueous solution A review. *Science Of The Total Environment* **2019**, 694.
- 36. Banks, D.; Jun, B.-M.; Heo, J.; Her, N.; Park, C. M.; Yoon, Y., Selected advanced water treatment technologies for perfluoroalkyl and polyfluoroalkyl substances: A review. *Separation and Purification Technology* **2020**, *231*, 115929.
- 37. Ji, B.; Kang, P.; Wei, T.; Zhao, Y., Challenges of aqueous per- and polyfluoroalkyl substances (PFASs) and their foreseeable removal strategies. *Chemosphere* **2020**, *250*, 126316.
- 38. Ateia, M.; Alsbaiee, A.; Karanfil, T.; Dichtel, W., Efficient PFAS removal by amine-functionalized sorbents: critical review of the current literature. *Environmental Science & Technology Letters* **2019**, *6* (12), 688-695.
- 39. Choudhary, A.; Dong, D.; Tsianou, M.; Alexandridis, P.; Bedrov, D., Adsorption Mechanism of perfluorooctanoate on cyclodextrin-based polymers: probing the synergy of electrostatic and hydrophobic interactions with molecular dynamics simulations. *ACS Materials Letters* **2022**, *4*, 853-859.

- 40. Gianni, P.; Barghini, A.; Bernazzani, L.; Mollica, V.; Pizzolla, P., Aggregation of cesium perfluorooctanoate on poly(ethylene glycol) oligomers in water. *Journal of Physical Chemistry B* **2006**, *110* (18), 9112-9121.
- 41. Gianni, P.; Barghini, A.; Bernazzani, L.; Mollica, V., Calorimetric investigation of the interaction between lithium perfluorononanoate and poly(ethylene glycol) oligomers in water. *Langmuir* **2006**, *22* (19), 8001-8009.
- 42. Bernazzani, L.; Gianni, P.; Mollica, V., Calorimetric study of the aggregation of lithium perfluorohexanoate on poly(ethyleneglycol) oligomers in water. *Journal of Solution Chemistry* **2010**, *39* (11), 1698-1709.
- 43. Wang, C.; Jin, C.; Yan, P.; Xiao, J.; Zhao, K., Effect of counterions on the interactions between perfluorooctanoate and polymers. *Acta Chimica Sinica* **2009**, *67* (19), 2159-2164.
- 44. Bernazzani, L.; Borsacchi, S.; Catalano, D.; Gianni, P.; Mollica, V.; Vitelli, M.; Asaro, F.; Feruglio, L., On the interaction of sodium dodecyl sulfate with oligomers of poly(ethylene glycol) in aqueous solution. *Journal of Physical Chemistry B* **2004**, *108* (26), 8960-8969.
- 45. Kancharla, S.; Choudhary, A.; Davis, R. T.; Dong, D.; Bedrov, D.; Tsianou, M.; Alexandridis, P., GenX in water: interactions and self-assembly. *Journal of Hazardous Materials* **2022**, *428*, 128137.
- 46. Kancharla, S.; Canales, E.; Alexandridis, P., Perfluorooctanoate in aqueous urea solutions: micelle formation, structure, and microenvironment. *International Journal of Molecular Sciences* **2019**, *20* (22), 5761.

- 47. Gjerde, M. I.; Nerdal, W.; Høiland, H., Interactions between poly(ethylene oxide) and sodium dodecyl sulfate as studied by NMR, conductivity, and viscosity at 283.1–298.1 K. *Journal of Colloid and Interface Science* **1998**, *197* (2), 191-197.
- 48. Minatti, E.; Zanette, D., Salt effects on the interaction of poly(ethylene oxide) and sodium dodecyl sulfate measured by conductivity. *Colloids and Surfaces A: Physicochemical and Engineering Aspects* **1996**, *113* (3), 237-246.
- 49. Dong, D.; Kancharla, S.; Hooper, J.; Tsianou, M.; Bedrov, D.; Alexandridis, P., Controlling the self-assembly of perfluorinated surfactants in aqueous environments. *Physical Chemistry Chemical Physics* **2021**, *23* (16), 10029-10039.
- 50. Berr, S. S.; Jones, R. R. M., Small-angle neutron scattering from aqueous solutions of sodium perfluorooctanoate above the critical micelle concentration. *Journal of Physical Chemistry* **1989**, *93* (6), 2555-2558.
- 51. Burkitt, S. J.; Ottewill, R. H.; Hayter, J. B.; Ingram, B. T., Small angle neutron scattering studies on micellar systems part 1. Ammonium octanoate, ammonium decanoate and ammonium perfluorooctanoate. *Colloid & Polymer Science* **1987**, *265* (7), 619-627.
- 52. Iijima, H.; Kato, T.; Yoshida, H.; Imai, M., Small-angle X-ray and neutron scattering from dilute solutions of cesium perfluorooctanoate. Micellar growth along two dimensions. *Journal of Physical Chemistry B* **1998**, *102* (6), 990-995.
- 53. Kancharla, S.; Dong, D.; Bedrov, D.; Tsianou, M.; Alexandridis, P., Structure and interactions in perfluorooctanoate micellar solutions revealed by small-angle neutron scattering and molecular dynamics simulations studies: Effect of urea. *Langmuir* **2021**, *37* (17), 5339-5347.

- 54. Kancharla, S.; Jahan, R.; Bedrov, D.; Tsianou, M.; Alexandridis, P., Role of chain length and electrolyte on the micellization of anionic fluorinated surfactants in water. *Colloids and Surfaces A: Physicochemical and Engineering Aspects* **2021**, *628*, 127313.
- 55. Krogstad, D. V.; Choi, S.-H.; Lynd, N. A.; Audus, D. J.; Perry, S. L.; Gopez, J. D.; Hawker, C. J.; Kramer, E. J.; Tirrell, M. V., Small angle neutron scattering study of complex coacervate micelles and hydrogels formed from ionic diblock and triblock copolymers. *Journal of Physical Chemistry B* **2014**, *118* (45), 13011-13018.
- 56. Padsala, S.; Patel, V. I.; Ray, D.; Aswal, V. K.; Bahadur, P., Mixed micelles of sodium perfluorooctanoate and imidazolium based ionic liquids in aqueous solution: A SANS and Tensiometric study. *Journal of Molecular Liquids* **2021**, *322*, 114558.
- 57. Hammouda, B.; Ho, D. L., Insight into chain dimensions in PEO/water solutions. *Journal of Polymer Science Part B: Polymer Physics* **2007**, *45* (16), 2196-2200.
- 58. Lancz, G.; Avdeev, M. V.; Petrenko, V. I.; Garamus, V. M.; Koneracka, M.; Kopcansky, P., SANS study of poly(ethylene glycol) solutions in D2O. *Acta Physica Polonica, A* **2010,** *118* (5), 980-982.
- 59. Hammouda, B.; Ho, D. L.; Kline, S., Insight into clustering in poly(ethylene oxide) solutions. *Macromolecules* **2004**, *37* (18), 6932-6937.
- 60. Srinivasan, V.; Blankschtein, D., Prediction of conformational characteristics and micellar solution properties of fluorocarbon surfactants. *Langmuir* **2005**, *21* (4), 1647-1660.
- 61. Ohtaki, H.; Radnai, T., Structure and dynamics of hydrated ions. *Chemical Reviews* **1993**, 93 (3), 1157-1204.

- 62. Singh, G.; Verma, R.; Wagle, S.; Gadre, S. R., Explicit hydration of ammonium ion by correlated methods employing molecular tailoring approach. *Molecular Physics* **2017**, *115* (21-22), 2708-2720.
- 63. Duvoisin, S.; Kuhnen, C. A.; Ouriques, G. R., Theoretical study of the ammonium perfluorooctanoate/water system. *Journal of Molecular Structure: Theochem* **2002**, *617* (1), 201-207.
- 64. Borodin, O., Polarizable force field development and molecular dynamics simulations of ionic liquids. *Journal of Physical Chemistry B* **2009**, *113* (33), 11463-11478.
- 65. Hoover, W. G., Canonical dynamics: Equilibrium phase-space distributions. *Physical Review A* **1985**, *31* (3), 1695-1697.
- 66. Yeh, I. C.; Berkowitz, M. L., Ewald summation for systems with slab geometry. *Journal of Chemical Physics* **1999**, *111* (7), 3155-3162.
- 67. Palmer, B. J., Direct application of SHAKE to the velocity Verlet algorithm. *Journal of Computational Physics* **1993**, *104*, 470-472.
- 68. Ortona, O.; D'Errico, G.; Paduano, L.; Sartorio, R., Ionic surfactant–polymer interaction in aqueous solution. *Physical Chemistry Chemical Physics* **2002**, *4* (12), 2604-2611.
- 69. Sesta, B.; Segre, A. L.; D'Aprano, A.; Proietti, N., 1H NMR, surface tension, viscosity, and volume evidence of micelle–polymer hydrophobic interactions: LiPFN–PVP system. *Journal of Physical Chemistry B* **1997**, *101* (2), 198-204.
- 70. Smith, G. D.; Bedrov, D., A Molecular dynamics simulation study of the influence of hydrogen-bonding and polar interactions on hydration and conformations of a poly(ethylene oxide) oligomer in dilute aqueous solution. *Macromolecules* **2002**, *35* (14), 5712-5719.

- 71. Cabane, B., Structure of some polymer-detergent aggregates in water. *Journal of Physical Chemistry* **1977**, *81* (17), 1639-1645.
- 72. Koda, Y.; Terashima, T.; Sawamoto, M., Fluorous microgel star polymers: selective recognition and separation of polyfluorinated surfactants and compounds in water. *Journal of American Chemical Society* **2014**, *136* (44), 15742-15748.
- 73. Tan, X.; Zhong, J.; Fu, C.; Dang, H.; Han, Y.; Král, P.; Guo, J.; Yuan, Z.; Peng, H.; Zhang, C.; Whittaker, A. K., Amphiphilic perfluoropolyether copolymers for the effective removal of polyfluoroalkyl substances from aqueous environments. *Macromolecules* **2021**, *54* (7), 3447-3457.